



Title	Effect of fuel ratio of coal on the turbulent flame speed of ammonia/coal particle cloud co-combustion at atmospheric pressure
Author(s)	Hadi, Khalid; Ichimura, Ryo; Hashimoto, Genya; Xia, Yu; Hashimoto, Nozomu; Fujita, Osamu
Citation	Proceedings of The Combustion Institute, 38(3), 4131-4139 https://doi.org/10.1016/j.proci.2020.06.358
Issue Date	2021-04-10
Doc URL	http://hdl.handle.net/2115/86802
Rights	© <2021>. This manuscript version is made available under the CC-BY-NC-ND 4.0 license http://creativecommons.org/licenses/by-nc-nd/4.0/
Rights(URL)	http://creativecommons.org/licenses/by-nc-nd/4.0/
Type	article (author version)
File Information	submitted unmarked.pdf



[Instructions for use](#)

[Title Page]

1. Effect of fuel ratio of coal on the turbulent flame speed of ammonia/coal particle cloud combustion at atmospheric pressure.

2. Author (s) : Khalid Hadi^{a,b,*}, Ryo Ichimura^a, Genya Hashimoto^a, Yu Xia^a, Nozomu Hashimoto^a,
Osamu Fujita^a

*^aDivision of Mechanical and Space Engineering, Hokkaido University,
Kita13 Nishi8, Kita-ku, Sapporo 060-8628, Japan.*

*^bMechanical Engineering Department,
Politeknik Sultan Azlan Shah, Behrang 35950, Perak, Malaysia.*

3. Corresponding author information:

Hadi bin Khalid*

Lecturer, Politeknik Sultan Azlan Shah,

Behrang 35950, Perak, Malaysia.

E-mail address: hadi.psa@gmail.com

Tel.: +6014 907 6052; Fax: +605 454 4993

4. Colloquium : Solid fuel combustion

5. Total length of paper : 6198 (word count via method 1)

6. List word equivalent lengths

Body: 3367

Equations: 0

References: 559

Table: 167

Figures: 2105 [160 +448 +190 +244+512+551 (for Fig. 1-6 with captions)]

7. Affirmation to pay color reproduction charges (if applicable) : No

8. Supplemental material : Available

Abstract

This study aims to clarify the effect of fuel ratio of coal on the turbulent flame speed of ammonia/coal particle cloud co-combustion at atmospheric pressure under various turbulence intensities. High-fuel-ratio coals are not usually used in coal-fired thermal power plants because of their low flame stability. The expectation is that ammonia as a hydrogen-energy carrier would improve the ignition capability of coal particles in co-combustion. Experiments on spherical turbulent flame propagation of co-combustion were conducted for various coal types under various turbulence intensities, using the unique experimental apparatus developed for the co-combustion. Experimental results show that the flame speed of co-combustion with a low equivalence ratio of ammonia/oxidizer mixture for bituminous coal case was found to be three times faster than that of pure coal combustion and two times faster than that of pure ammonia combustion. On the other hand, the flame speed of co-combustion for the highest-fuel-ratio coal case is lower than that of the pure ammonia combustion case, although the flame propagation can be sustained due to the ammonia mixing. To explain the difference of tendencies depending on the fuel ratio of coal, a flame propagation mechanism of ammonia/coal particle cloud co-combustion was proposed. Two positive effects are the increases of local equivalence ratio and the increases of radiation heat flux, which increases the flame speed. In opposite, a negative effect is the heat sink effect that decreases the flame speed. The two positive effects on the flame speed of co-combustion overwhelm a negative effect for bituminous coal case, while the negative effect overcomes both positive effects for the highest-fuel-ratio coal case. The findings of the study can contribute to the reduction of solid fuel costs when the ammonia is introduced as CO₂ free energy carrier and can improve the energy security through the utilization of high-fuel-ratio coals.

* Corresponding author: Tel.: +6014 907 6052. E-mail address: hadi.psa@gmail.com

Keywords: Ammonia; coal combustion; co-combustion; high-fuel-ratio coal; flame speed

List of figure captions

Figure 1	Schematic of experimental apparatus.
Figure 2	Raw flame images of ammonia/coal particle cloud co-combustion transformed to binary images.
Figure 3	The sequence of flame propagation images of pure coal, ammonia/coal particle co-combustion, and pure ammonia combustion, at $u' = 0.32$ m/s.
Figure 4	Flame radius as a function of elapsed time of ammonia/coal particle cloud co-combustion for C5 and UL coal, and pure ammonia combustion, at $u' = 0.65$ m/s. #1, #2 and #3 indicate the experimental numbers of repeated tests.
Figure 5	Relationship between flame speed and turbulence intensity, u' of ammonia/coal particle cloud co-combustion, pure coal, and pure ammonia combustion.
Figure 6	A mechanism of flame propagation of ammonia/coal particle cloud co-combustion.

1. Introduction

Coal is widely used for energy generation because of its abundant supply from accessible deposits worldwide. In fact, coal is a crucial energy source among the fossil fuels in the electricity generation industry. However, at least in Japan, high-fuel-ratio coals were not used in coal-fired boilers in thermal power plants. This is because their flame speeds were very low or flame propagation could not be sustained. In a coal-fired boiler, flame speed is one of the most important parameters of flame stability in the burner [1].

Utilizing ammonia in a coal-fired thermal power plant is a promising alternative because ammonia can be directly burned in the burner. Ammonia is a carbon-free fuel and has a relatively high hydrogen content [2]. Additionally, the storage and transportation of ammonia are relatively easy compared to hydrogen [3]. Furthermore, a new method for ammonia production has been developed to realize ammonia as a renewable fuel. Recently, many researchers have studied the flame propagation behavior of ammonia because of its high potential as an energy carrier [2-8]. Although the mixing combustion of coal and ammonia is already studied by some researchers [9], the detailed effect of ammonia addition for the flame propagation characteristics, which is important to control the flame stability, has not been investigated yet.

Previously, flame propagation of pulverized coal clouds in a quiescent environment was clarified in many studies [1,10-11]. Taniguchi et al. [12] suggested that the pyrolysis rate and the amount of volatile matter generated strongly affected the flame stability. Generally, gaseous fuel flame propagation is faster than that of coal particles. Therefore, the pyrolysis rate of coal particles can be increased by heat transfer from flame propagation of ammonia with the addition of volatile matter in ammonia/coal particle cloud co-combustion. Hadi et al. [13] suggested that the increase of turbulent heat transfer increased the flame propagation velocity of coal particle clouds. Volatile combustion has been investigated by many researchers [14-19]. Reith et al. [20] suggested that different particles experienced very different heat-up rates, which could even affect flame stabilization. The mean volatile

combustion duration increased when the diameters of the particles increased [15]. Soot formation affected the flame propagation behavior in coal clouds [21-26]. Hashimoto et al. [24] and Hayashi et al. [25] explored soot formation characteristics in a lab-scale turbulent pulverized coal flame. The radiation from soot was able to increase the pyrolysis rate of coal particles. Due to the presence of soot, the volatile flame duration was extended [27]. The addition of gaseous fuel for co-combustion also has previously been studied. Xia et al. [28] studied coal/methane/air mixture combustion in a strained flow configuration. However, the authors are not aware of any previous papers that have reported the fundamental mechanism of ammonia/coal particle cloud co-combustion.

The present study aims to clarify the effect of fuel ratio of coal on the turbulent flame speed of ammonia/coal particle cloud co-combustion at atmospheric pressure under various turbulence intensities. The most significant part of the study is the investigation of the ignition capability of high-fuel-ratio coal particles by using ammonia as an energy carrier. Based on our experimental results, the flame propagation mechanism is suggested for further study of ammonia/coal particle cloud co-combustion.

2. Experimental apparatus and procedures

Experiments on pure coal combustion, pure ammonia combustion, and ammonia/coal particle cloud co-combustion were conducted using a constant volume spherical inner combustion chamber, as shown in Fig. 1. The inner spherical diameter was 200 mm and the total volume of the chamber was approximately $6.2 \times 10^{-3} \text{ m}^3$. Pulverized coal particles of common bituminous coal (C5) and high-fuel-ratio coals (TW, KK, and UL) were used as fuel. Table 1 shows the properties of these coals. Four kinds of coal whose fuel ratios are ranged from 1.56 to 5.3 were used. Fuel ratio is the ratio of fixed carbon to volatile matter. In coal-O₂ N₂ (pure coal) cloud combustion, NH₃ -O₂ N₂ (pure ammonia) combustion, and NH₃ -O₂ N₂ -coal (ammonia/coal particle) cloud co-combustion, diluted oxygen (40 vol% O₂ and 60 vol% N₂) was used as the ambient gas, similar to the pure coal combustion [13]. The

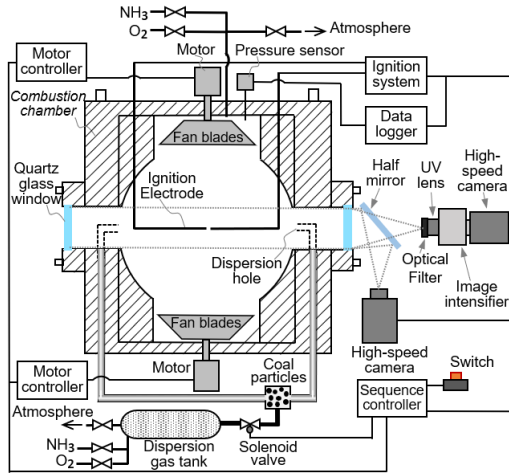


Fig. 1. Schematic of experimental apparatus.

Table 1
Properties of coals.

Analysis	Bituminous coal		High-fuel-ratio coal	
	C5	TW	KK	UL
Proximate [wt%]				
Moisture ^b	0.7	2.3	0.3	3.0
Ash ^a	14.2	19.9	12.9	21.2
Volatile matter ^a	33.5	22.9	20.9	12.5
Fixed carbon ^a	52.3	57.2	66.2	66.3
Fuel ratio	1.56	2.5	3.17	5.3
Ultimate [wt%, dry]				
Carbon	70.5	69.2	76.7	71.8
Hydrogen	4.64	3.64	4.09	2.48
Nitrogen	1.66	1.54	1.31	1.52
Oxygen	8.59	5.4	3.6	2.8
Sulfur	0.46	0.41	1.46	0.34
Heating value [MJ/kg]	27.8	27.2	30.1	27.2
Mean particle size [μm]	48	48	33	42

^aDry basis.

^bAs received.

flame propagation behavior of ammonia/coal particle cloud co-combustion was simultaneously recorded by direct imaging and OH radical imaging through the same window, as shown in Fig. 1. A half mirror was employed for simultaneously recording direct and OH radical imaging. An image intensifier equipped with a 300 nm bandwidth filter and a UV lens was used for OH radical imaging with precise timing to provide readable OH radical images for analysis.

Experiments on ammonia/coal particle cloud co-combustion were performed for coal concentration, $G = 0.6 \text{ kg/m}^3$ and $\text{NH}_3\text{-O}_2\text{-N}_2$ (ammonia) at equivalence ratio, $\phi = 0.6$. The turbulence intensity was set as 0.32, 0.65, 0.97, and 1.29 m/s. In C5 pure coal combustion, $G = 0.6 \text{ kg/m}^3$ was the lowest coal concentration that sustained flame propagation in all tested turbulence intensities. Therefore, $G = 0.6 \text{ kg/m}^3$ was selected in the present study. Additionally, the lean condition of the ammonia mixture was selected. In this type of co-combustion, the gaseous flame front that comprises ammonia and volatile matter is called “reaction front”. Therefore, to capture the OH radical signals from the gaseous fuel flame edge, OH radical imaging was employed to obtain the reaction front of co-combustion. Direct imaging was employed to obtain the luminous flame.

The ammonia mixture was prepared inside the chamber and the dispersion tank. The pressure inside the tank was 300 kPa. The mixture inside the chamber was set to -25 kPa to allow the dispersion gas mixture that carries the coal particles to achieve the atmospheric pressure (0.1 MPa) after

dispersion. The mixture was ignited at atmospheric pressure by using a spark ignitor with spark energy of 5.5 J. On the top view of chamber, four 10-mm diameter dispersion holes are in the cross configuration on the chamber body, for coal particle's dispersion. Therefore, on the top view, the axes of dispersion holes and the observation windows look like a regular octagon. On the vertical axis of the combustion field, the four dispersion holes of coal particles were at the middle level which is the same level as the spark ignition point. Generally, this is to target the coal particle's dispersion to the center of the sphere.

Counter-rotation of two identical fans was employed to generate a turbulent flow field inside the chamber. The correlation between the fan rotational speed, N , and turbulence intensity, u' was obtained from particle image velocimetry (PIV) measurements [13]. The pressure inside the chamber was measured using a Valcom VPRTF-A4 pressure sensor and recorded via a data logger. Another similar pressure sensor was employed to monitor gas pressure inside the dispersion tank.

The results of ammonia/coal particle cloud co-combustion were compared to those of pure ammonia combustion. In pure ammonia combustion, the equivalence ratio, ϕ , of NH_3 - O_2 - N_2 (ammonia) was 0.6, which was the same consideration in the gas composition during the ammonia/coal particle cloud co-combustion. A minimum of three experimental data sets for each condition was used for the analysis. In the ammonia/coal particle cloud co-combustion, the error of coal concentration was $\pm 3\%$ [weight %]. The present study aims to introduce the ammonia in practical coal-fired boilers, therefore based on thermal input, the equivalent amount of coal particles were subtracted when the ammonia was added. Table S1 shows the final coal concentration for co-combustion after ammonia was added (see Appendix A).

3. Results and discussion

In pure coal combustion, the bituminous coal (C5) sustained flame propagation in all tested turbulence intensities [13]. However, in the high-fuel-ratio coals cases, only TW coal sustained flame

propagation in high turbulence intensities with a 25% probability, while the KK and UL coals did not sustain flame propagation in all tested turbulence intensities.

In pure ammonia combustion, both OH radical imaging and Schlieren photography was employed. The Schlieren photography method can capture positions having high gradients of gas densities, while OH radical imaging can capture OH radical signal during the flame propagation. A comparison of the two methods was indicated that overall, both of them showed very similar results. However, Schlieren photography could not be implemented for the gaseous flame in co-combustion because of the presence of the coal particle cloud. Therefore, only data from OH radical imaging is shown later.

Figure 2 shows the simultaneous images at the same elapsed time of (a) direct imaging and (b) OH radical imaging in ammonia/coal particle cloud co-combustion for C5 coal, at $u' = 0.32$ m/s. The direct imaging was used to detect luminous flame front, when the number density of the soot particles, which are formed by the secondary pyrolysis of volatile matter evolved from coal particles, becomes sufficient, the luminous flame front was formed. The front detected by OH radical imaging

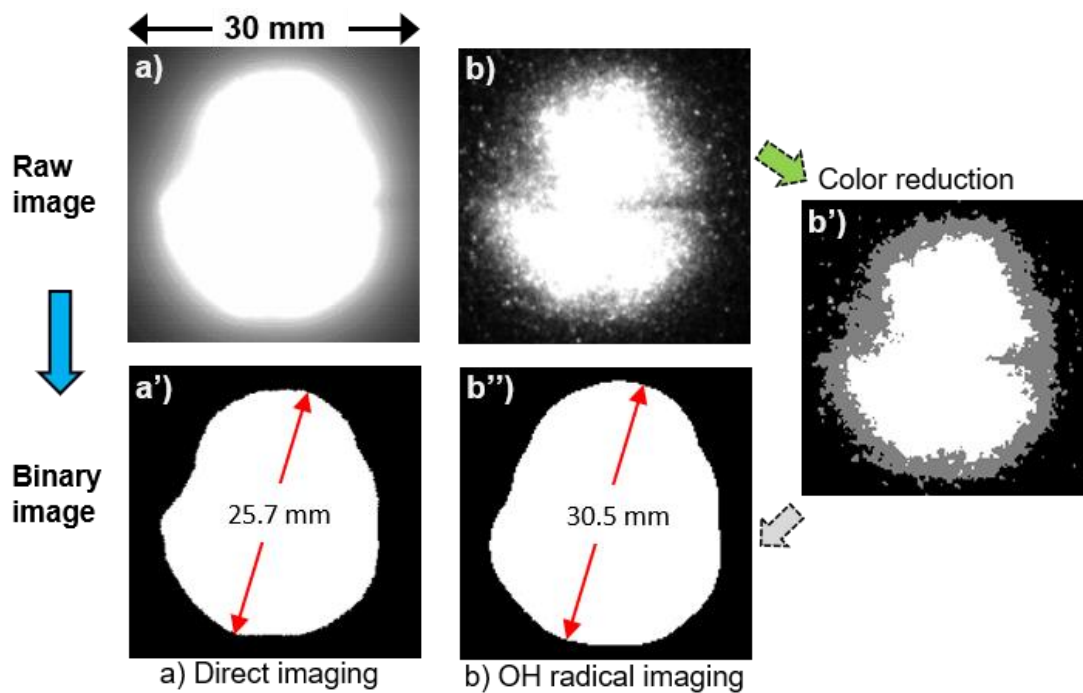


Fig. 2. Raw flame images of ammonia/coal particle cloud co-combustion transformed to binary images.

is defined as the reaction front. To measure the flame diameter, the colors of the OH radical images were reduced to enhance the visibility of the flame front. Figure 2(b') shows an example of the OH radical image after the color reduction. The raw images were transformed into binary images to show the measured flame front. As shown by the red arrows in Fig. 2, the flame radius was measured between the farthest flame fronts, which was the same procedure used in pure coal combustion [13].

The binary images of flame propagation were shown to compare the C5 coal in pure coal particle cloud combustion with ammonia/coal particle cloud co-combustion. Figure 3 shows the sequence of flame images for (a) direct imaging of pure coal combustion, (b) direct imaging of ammonia/coal particle co-combustion, (c) OH radical imaging of ammonia/coal particle co-combustion, and (d) OH radical imaging of pure ammonia combustion, at $u' = 0.32$ m/s. At the same elapsed time of 10 ms, the flame image of pure coal combustion is a relatively small scale compared with the luminous flame (direct imaging) in the co-combustion. Additionally, the ammonia flame in pure ammonia combustion is a relatively small scale compared with the reaction front (OH radical imaging) in co-combustion. It confirms that the flame speed in co-combustion is relatively higher compared with pure coal and pure ammonia combustions.

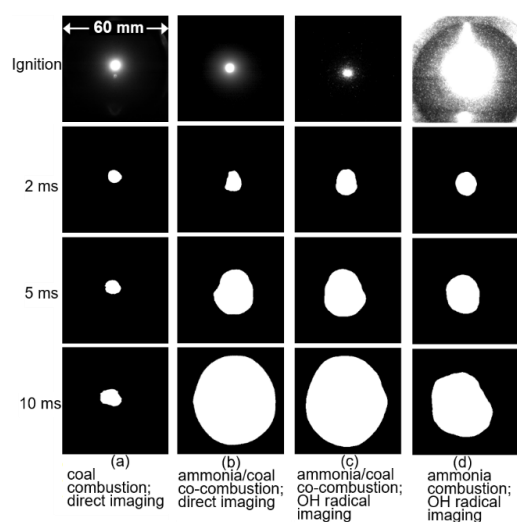


Fig. 3. The sequence of flame propagation images of pure coal, ammonia/coal particle co-combustion, and pure ammonia combustion, at $u' = 0.32$ m/s.

Figure 4 shows the radii histories of both flames that were measured using direct imaging (“Direct”) and OH radical imaging (“OH”) for bituminous coal (C5) and high-fuel-ratio coal (UL) in ammonia/coal particle cloud co-combustion, and pure ammonia combustion measured by OH radical imaging (“OH_NH₃”), at $u' = 0.65$ m/s. In ammonia/coal particle cloud co-combustion for C5 coal, the radii of reaction front from OH radical imaging are slightly larger than luminous flame front those from direct imaging, for all of the cases. However, in ammonia/coal particle cloud co-combustion for UL coal, it showed a considerable difference. It showed for all cases, the radii of the reaction front were considerably larger than the luminous flame front. The results illustrate that the fuel ratio of coal determines the different flame propagation behavior of bituminous coal and the high-fuel-ratio coal in ammonia/coal particle cloud co-combustion. Moreover, the radii of pure ammonia flame are smaller than ammonia/coal particle cloud co-combustion for C5 coal case, but larger than ammonia/coal

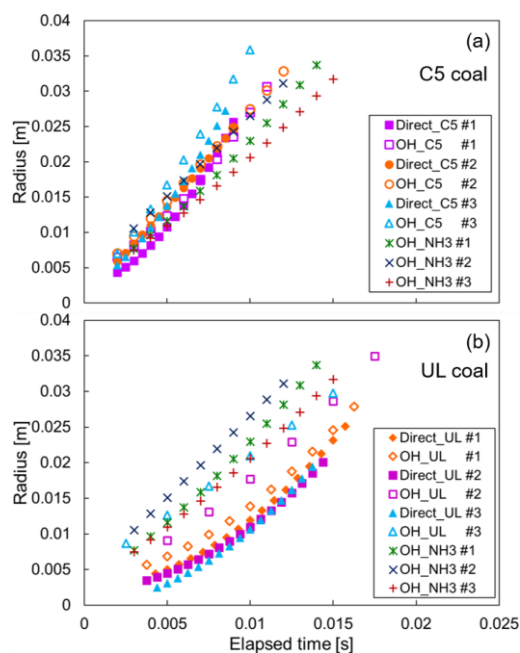


Fig. 4. Flame radius as a function of elapsed time of ammonia/coal particle cloud co-combustion for C5 and UL coal, and pure ammonia combustion, at $u' = 0.65$ m/s. #1, #2 and #3 indicate the experimental numbers of repeated tests.

particle cloud co-combustion for UL coal case. The flame radii were measured 2 ms after the spark ignition until the maximum scale of the flame reached the edge of the window. The flame speed was obtained from the relationship of flame radius and elapsed time, which was a similar approach to [13].

Figure 5 shows the flame speed as a function of turbulence intensity for ammonia/coal particle cloud co-combustion for (a) C5, (b) TW, (c) KK, and (d) UL coals. In Fig. 5, the flame speeds at flame radius of 10.45 mm, which were calculated by the reaction front radius histories, are shown, the same approach as [13]. For all coal cases, the flame speeds increase with increasing turbulence intensity. This tendency is because of the increase of the flame front area and the increase of the turbulent heat transfer rate at the flame front as the turbulence intensity increases, as described in [13]. For C5 coal case (Fig. 5 (a)), for all turbulence intensities, the flame speeds of ammonia/coal particle cloud co-combustion are approximately three times faster than that of the pure coal combustion. Additionally, it is approximately two times faster than that of pure ammonia combustion. On the other hand, the difference in flame speed between ammonia/coal co-combustion and pure ammonia combustion is small for high-fuel-ratio coal (TW, KK, UL) cases. Especially, the flame speed of the ammonia/coal co-combustion for UL coal case is lower than that of the pure ammonia combustion case. These different tendencies depending on coal types, are caused by the difference of volatile matter amount in the coal particles, as discussed in the followings.

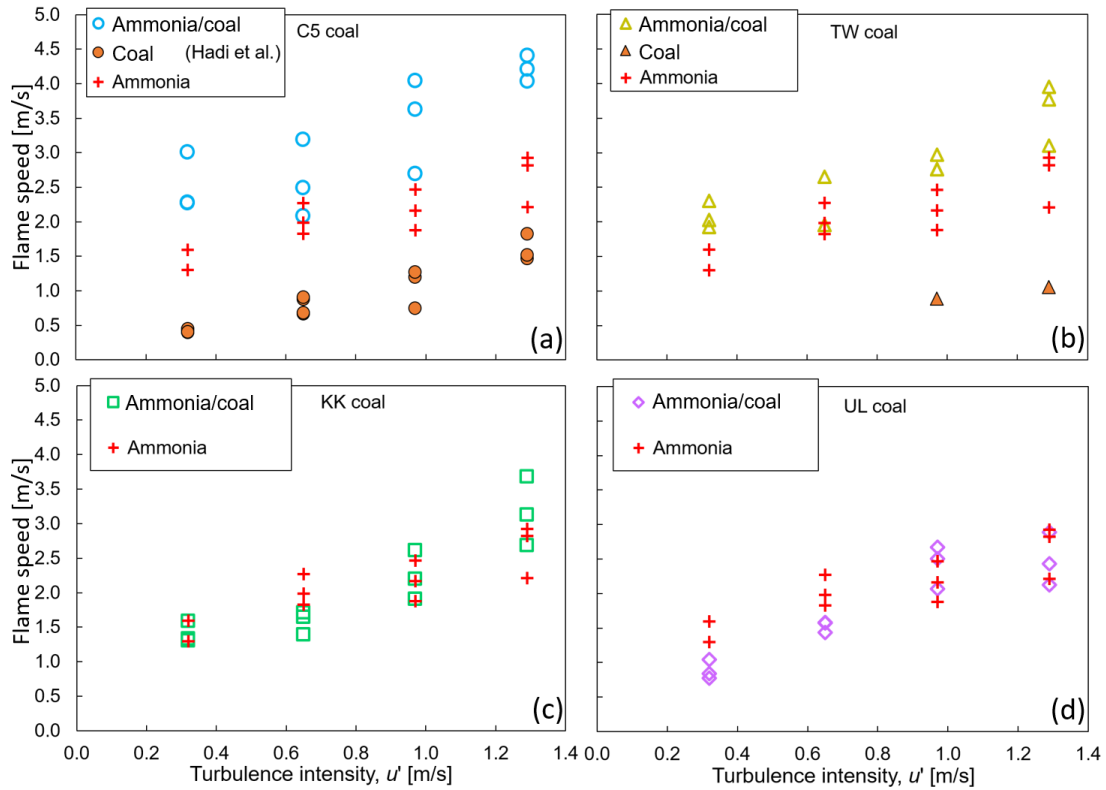


Fig. 5. Relationship between flame speed and turbulence intensity, u' of ammonia/coal particle cloud co-combustion, pure coal, and pure ammonia combustion.

Figure 6 shows the mechanism of flame propagation of ammonia/coal particle cloud co-combustion proposed by the authors. The particle diameter is ranging from 1 to 220 μm for all coal types. The particles with different particle diameters are illustrated in Fig. 6. At the first pyrolysis near the reaction front, the volatile matter release rate of small particles is relatively faster (illustrated by the higher gradient-longer blue arrow in Fig. 6 (a) and (b)). The amount of volatile matter released from C5 is larger (thick blue arrow in Fig. 6(a)) than UL coal (thin blue arrow in Fig. 6(b)) during the preheat and the second pyrolysis near the luminous flame front. In addition, char combustion starts subsequently at the post-reaction front. Char combustion of small particles start faster than the larger

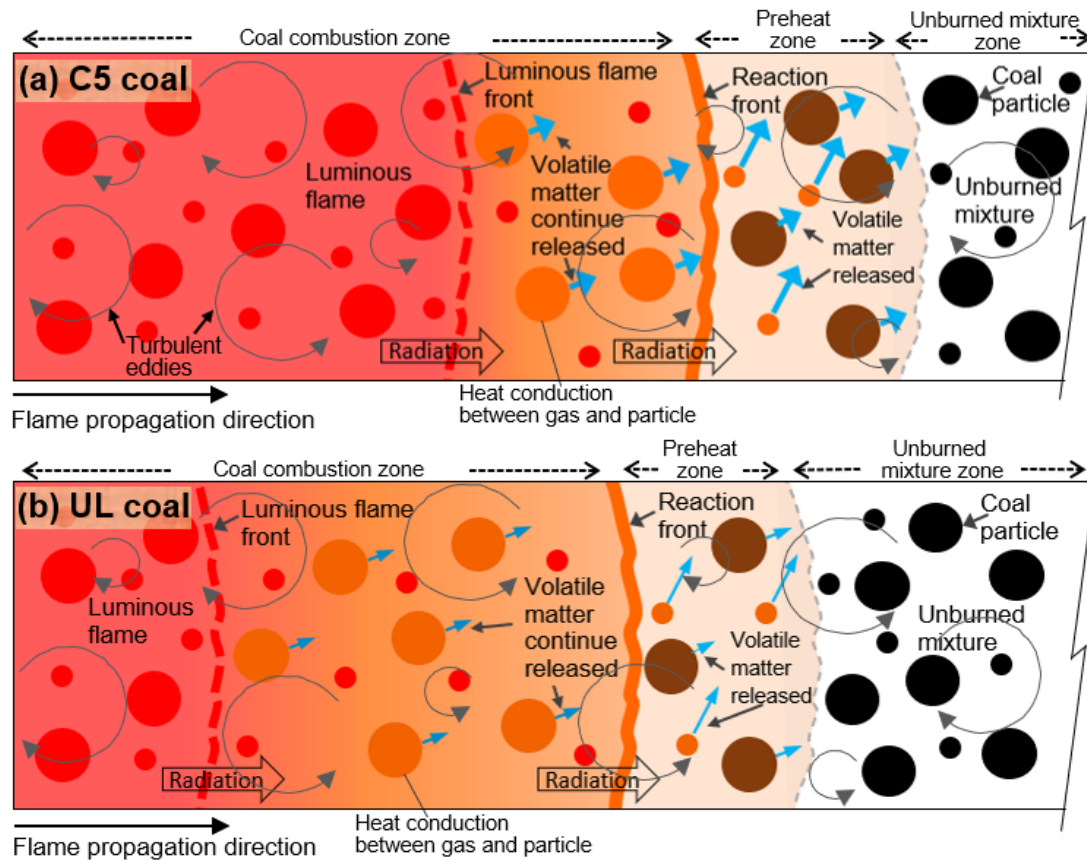


Fig. 6. A mechanism of flame propagation of ammonia/coal particle cloud co-combustion.

diameter particles at the post-reaction front. In the ammonia/coal particle cloud co-combustion field, the unburned coal particles in front of the reaction front are preheated (preheat zone in Fig. 6) by the convection and radiation effects. The volatile matter is evolved from coal particles in this preheat zone. Therefore, both ammonia and volatile matter are combusted in the narrow area of reaction front as the gaseous reaction. Because of the addition of the volatile matter to ammonia in the preheat zone, the local equivalence ratio is increased, and this effect acts as a positive effect for the speed of the reaction front for ammonia lean mixture case. This volatile addition effect can be a negative effect if the equivalence ratio of ammonia/oxidizer is fuel rich condition. The effect of the equivalence ratio of ammonia/oxidizer was investigated by Xia et al. [29], and it is beyond the scope of this paper. In

addition to the effect of local equivalence ratio increase, the radiation from the luminous flame to the solid particles in the preheat zone can assist the preheating of the coal particles [30]. On the other hand, the solid particles in the preheat zone act as a heat sink, and this can be a negative effect on the speed of the reaction front. These three kinds of effects are competed to determine the flame speed of ammonia/coal particle cloud co-combustion.

In the case of C5 coal as shown in Fig. 6 (a), the amount of volatile matter in coal particles is larger than that for high-fuel-ratio coal cases. Because of this, the addition of the volatile matter amount evolved in front of the reaction front for C5 coal case is larger than that for other cases. In addition to that, the distance between the reaction front and the luminous flame front for C5 coal is shorter as illustrated in Fig. 6 (a). It should be noted that this short distance for C5 coal was confirmed in Fig. 4 (a). Because of the sufficient amount of the volatile matter in the reaction front, the soot formation on the post-reaction front is faster for C5 case. Consequently, the distance between the reaction front and the luminous flame front is short for C5 coal case. Due to the short distance between the reaction front and the luminous flame front, the coal particles in the preheat zone receive the larger radiation heat flux. Subsequently, the first positive effect, which is the sufficient increase in local equivalence ratio, and the second positive effect, which is the higher radiation heat flux from the luminous flame, overcome the negative effect, which is the heat sink effect of coal particles in preheat zone. Due to the overwhelming positive effects, the flame speed of ammonia/coal particle co-combustion for C5 coal case is much higher than that of pure ammonia combustion as observed in Fig. 5 (a).

On the other hand, the amount of volatile matter addition in front of the reaction front for high-fuel-ratio coals is lower than that for bituminous coal (C5). Moreover, the radiation heat flux from the luminous flame to coal particles in the preheat zone for the high-fuel-ratio coal cases is lower than that for C5 case. This is caused by the long distance between the reaction front and the luminous flame front as illustrated in Fig. 6(b). Because the volatile matter content is lesser in the high-fuel-ratio coal particles, the volatile release rate is also lower resulting in a slower soot formation rate. Consequently, the luminous flame front is relatively far from the reaction front. It should be noted that the long distance between the reaction front and the luminous flame front for UL coal is confirmed in Fig. 4 (b). This longer distance results in lower radiation heat flux from the luminous flame to coal particles in the preheat zone. Because of the weakness of the first positive effect, which is the little increase in local equivalence ratio, and the weakness of second positive effect, which is the lower radiation heat flux from the luminous flame, the negative effect, which is the heat sink effect of coal particles in the preheat zone, overcome the both positive effects for UL coal case (the negative effect does not change significantly between all coal types due to similar values of coal particle specific heat). Due to the overwhelming of the negative effect, the flame speed of ammonia/coal particle co-combustion of UL coal case is lower than that of pure ammonia combustion as observed in Fig. 5 (d).

As described in Section 2, the equivalent amount of coal particles was subtracted when the ammonia was added. However, even if the ammonia is added without the subtraction of coal particles, it was suggested that the basic tendency of flame speed will not be changed, although the effect can be

enhanced little such as the flame speed of ammonia/C5 coal can be increased, compared to the present study.

4. Conclusions

In this study, experimental results of the turbulent flame speed of ammonia/coal particle cloud co-combustion at atmospheric pressure are reported for the first time. The effect of fuel ratio of coal on the flame speed of ammonia/coal particle cloud co-combustion under various turbulence intensities was clarified. The principal findings of this study are as follows:

- i. The distance between the reaction front and the luminous flame front is shorter for bituminous coal case, while that is longer for high-fuel-ratio coal cases. This is because a longer time is necessary for soot particle formation in high-fuel-ratio coal cases due to a low volatile matter release rate.
- ii. There are two positive effects on the flame speed of ammonia/coal particle cloud co-combustion with a lean equivalence ratio of ammonia/oxidizer mixture, which are the increase of local equivalence ratio because of the addition of volatile matter from coal particles and the increase of radiation heat flux from the luminous flame to coal particles in preheat zone. One negative effect is the heat sink effect because of the heat capacity of coal particles in the preheat zone.
- iii. For bituminous coal, the positive effects are considerable compared to the negative effect. On the other hand, the negative effect overshadowed both positive effects for the high-fuel-ratio coals.

5. Acknowledgment

Part of the present work was supported by JST Sakigake (PRESTO) Grant Number JPMJPR1542. The authors are indebted to Dr. Suda of IHI Co., Prof. Kitagawa of Kyushu Univ., Prof. Hayakawa of

Tohoku Univ. for their helpful advice and discussion. The authors also indebted to the Central Research Institute of Electric Power Industry for providing coal particle samples.

Appendix A. Supplementary data

Table S1	Final coal concentration for ammonia/coal particle cloud co-combustion.
----------	---

References

- [1] T. Suda, K. Masuko, J. Sato, A. Yamamoto, K. Okazaki, Effect of carbon dioxide on flame propagation of pulverized coal clouds in CO₂/O₂ combustion, *Fuel*. 86 (2007) 2008–2015.
- [2] A. Hayakawa, T. Goto, R. Mimoto, Y. Arakawa, T. Kudo, H. Kobayashi, Laminar burning velocity and Markstein length of ammonia/air premixed flames at various pressures, *Fuel*. 159 (2015) 98–106.
- [3] A. Ichikawa, A. Hayakawa, Y. Kitagawa, K.D. Kunkuma Amila Somarathne, T. Kudo, H. Kobayashi, Laminar burning velocity and Markstein length of ammonia/hydrogen/air premixed flames at elevated pressures, *Int. J. Hydrogen Energy*. 40 (2015) 9570–9578.
- [4] H. Kobayashi, A. Hayakawa, K.D.K.A. Somarathne, E.C. Okafor, Science and technology of ammonia combustion, *Proc. Combust. Inst.* 37 (2019) 109–133.
- [5] H. Nakamura, S. Hasegawa, Combustion and ignition characteristics of ammonia / air mixtures in a micro flow reactor with a controlled temperature profile, *Proc. Combust. Inst.* 36 (2017) 4217–4226.
- [6] H. Xiao, A. Valera-medina, P.J. Bowen, Study on premixed combustion characteristics of ammonia / methane fuels, *Energy*. 140 (2017) 125–135.
- [7] R. Ichimura, K. Hadi, N. Hashimoto, A. Hayakawa, H. Kobayashi, O. Fujita, Extinction limits of an ammonia/air flame propagating in a turbulent field, *Fuel*. 246 (2019) 178–186.
- [8] Y. Xia, G. Hashimoto, K. Hadi, N. Hashimoto, A. Hayakawa, Turbulent burning velocity of

ammonia / oxygen / nitrogen premixed flame in O₂-enriched air condition, *Fuel*. 268 (2020) 117383.

- [9] J. Zhang, T. Ito, H. Ishii, S. Ishihara, T. Fujimori, Numerical investigation on ammonia co-firing in a pulverized coal combustion facility: Effect of ammonia co-firing ratio, *Fuel* 267 (2020) 117166.
- [10] O. Fujita, Kenichi Ito, Takaharu Tagashira, Jun'ichi Sato, Measurement of flame propagation speed of coal dust cloud using a microgravity environment, *Heat Transf. Microgravity*. 269 (1993).
- [11] T. Kiga, S. Takano, N. Kimura, K. Omata, M. Okawa, T. Mori, M. Kato, Characteristics of pulverized-coal combustion in the system of oxygen/recycled flue gas combustion, *Energy Convers. Manag.* 38 (1997) S129–S134.
- [12] M. Taniguchi, H. Kobayashi, K. Kiyama, Y. Shimogori, Comparison of flame propagation properties of petroleum coke and coals of different rank, *Fuel*. 88 (2009) 1478–1484.
- [13] K. Hadi, R. Ichimura, N. Hashimoto, O. Fujita, Spherical turbulent flame propagation of pulverized coal particle clouds in an O₂/N₂ atmosphere, *Proc. Combust. Inst.* 37 (2019) 2935–2942.
- [14] J. Köser, L.G. Becker, A. Goßmann, B. Böhm, A. Dreizler, Investigation of ignition and volatile combustion of single coal particles within oxygen-enriched atmospheres using high-speed OH-PLIF, *Proc. Combust. Inst.* 36 (2017) 2103–2111.

- [15] J. Köser, T. Li, N. Vorobiev, A. Dreizler, M. Schiemann, B. Böhm, Multi-parameter diagnostics for high-resolution in-situ measurements of single coal particle combustion, *Proc. Combust. Inst.* 37 (2019) 2893–2900.
- [16] R. Knappstein, G. Kuenne, T. Meier, A. Sadiki, J. Janicka, Evaluation of coal particle volatiles reaction by using detailed kinetics and FGM tabulated chemistry, *Fuel*. 201 (2017) 39–52.
- [17] S. Farazi, A. Attili, S. Kang, H. Pitsch, Numerical study of coal particle ignition in air and, *Proc. Combust. Inst.* 37 (2019) 2867–2874.
- [18] L. Yao, C. Wu, Y. Wu, L. Chen, J. Chen, X. Wu, K. Cen, Investigating particle and volatile evolution during pulverized coal combustion using high-speed digital in-line holography, *Proc. Combust. Inst.* 37 (2019) 2911–2918.
- [19] H. Lee, S. Choi, An observation of combustion behavior of a single coal particle entrained into hot gas flow, *Combust. Flame*. 162 (2015) 2610–2620.
- [20] M. Rieth, A.G. Clements, M. Rabaçal, F. Proch, O.T. Stein, A.M. Kempf, Flamelet LES modeling of coal combustion with detailed devolatilization by directly coupled CPD, *Proc. Combust. Inst.* 36 (2017) 2181–2189.
- [21] O. Co, R. Khatami, Y.A. Levendis, M.A. Delichatsios, Soot loading , temperature and size of single coal particle envelope flames in conventional- and oxy-combustion conditions, *Combust. Flame*. 162 (2015) 2508–2517.
- [22] N. Hashimoto, H. Shirai, Numerical simulation of sub-bituminous coal and bituminous coal

- mixed combustion employing tabulated-devolatilization-process model, *Energy*. 71 (2014) 399–413.
- [23] H. Takahashi, N. Hashimoto, H. Watanabe, R. Kurose, O. Fujita, Prediction of soot formation characteristics in a pulverized- coal combustion field by large eddy simulations with the TDP model, *Proc. Combust. Inst.* 37 (2018) 1–9.
- [24] N. Hashimoto, J. Hayashi, N. Nakatsuka, K. Tainaka, S. Umemoto, H. TSUJI, F. Akamatsu, H. Watanabe, H. Makino, Primary soot particle distributions in a combustion field of 4 kW pulverized coal jet burner measured by time resolved laser induced incandescence (TiRe-LII), *J. Therm. Sci. Technol.* 11 (2016) JTST0049–JTST0049.
- [25] J. Hayashi, N. Hashimoto, N. Nakatsuka, H. Tsuji, H. Watanabe, H. Makino, F. Akamatsu, Soot formation characteristics in a lab-scale turbulent pulverized coal flame with simultaneous planar measurements of laser induced incandescence of soot and Mie scattering of pulverized coal, *Proc. Combust. Inst.* 34 (2013) 2435–2443.
- [26] J. Hayashi, N. Hashimoto, N. Nakatsuka, Simultaneous imaging of Mie scattering , PAHs laser induced fluorescence and soot laser induced incandescence to a lab-scale turbulent jet pulverized coal flame, *Proc. Combust. Inst.* 37 (2019) 3045–3052.
- [27] K. Xu, H. Zhang, Y. Wu, M. Baroncelli, H. Pitsch, Transient model for soot formation during the combustion of single coal particles, *Proc. Combust. Inst.* 36 (2017) 2131–2138.
- [28] M. Xia, D. Zabrodiec, P. Scouflaire, B. Fiorina, Experimental and numerical studies of

pulverized coal devolatilization and oxidation in strained methane / air flames, Proc. Combust.

Inst. 36 (2017) 2123–2130.

- [29] Y. Xia, K. Hadi, G. Hashimoto, N. Hashimoto, O. Fujita, Effect of ammonia/oxygen/nitrogen equivalence ratio on spherical turbulent flame propagation of pulverized coal/ammonia co-combustion, Proc. Combust. Inst. 38 (2020) (Under review).
- [30] H. Hanai, H. Kobayashi, T. Niioka, A numerical study of pulsating flame propagation in mixtures of gas and particles, Proc. Combust. Inst. 28 (2000) 815–822.

1. Ms. Ref. No.: PROCI-D-19-00715R1
 2. Author (s) : Khalid Hadi, Ryo Ichimura, Genya Hashimoto, Yu Xia, Nozomu Hashimoto, Osamu Fujita
 3. Title: Effect of fuel ratio of coal on the turbulent flame speed of ammonia/coal particle cloud co-combustion at atmospheric pressure.
- Proceedings of The Combustion Institute

Figures in gray scale version.

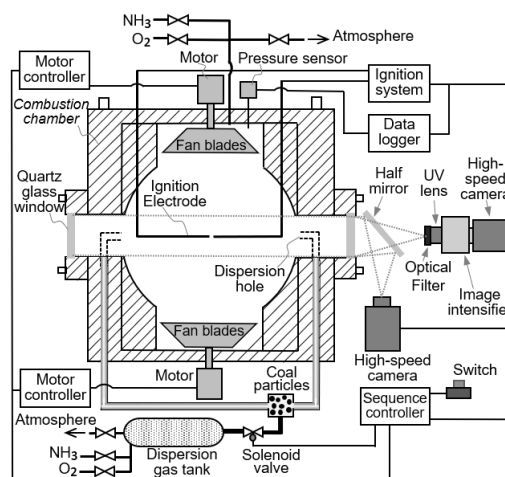


Fig. 1. Schematic of experimental apparatus.

1. Ms. Ref. No.: PROCI-D-19-00715R1
2. Author (s) : Khalid Hadi, Ryo Ichimura, Genya Hashimoto, Yu Xia, Nozomu Hashimoto, Osamu Fujita
3. Title: Effect of fuel ratio of coal on the turbulent flame speed of ammonia/coal particle cloud co-combustion at atmospheric pressure.
Proceedings of The Combustion Institute

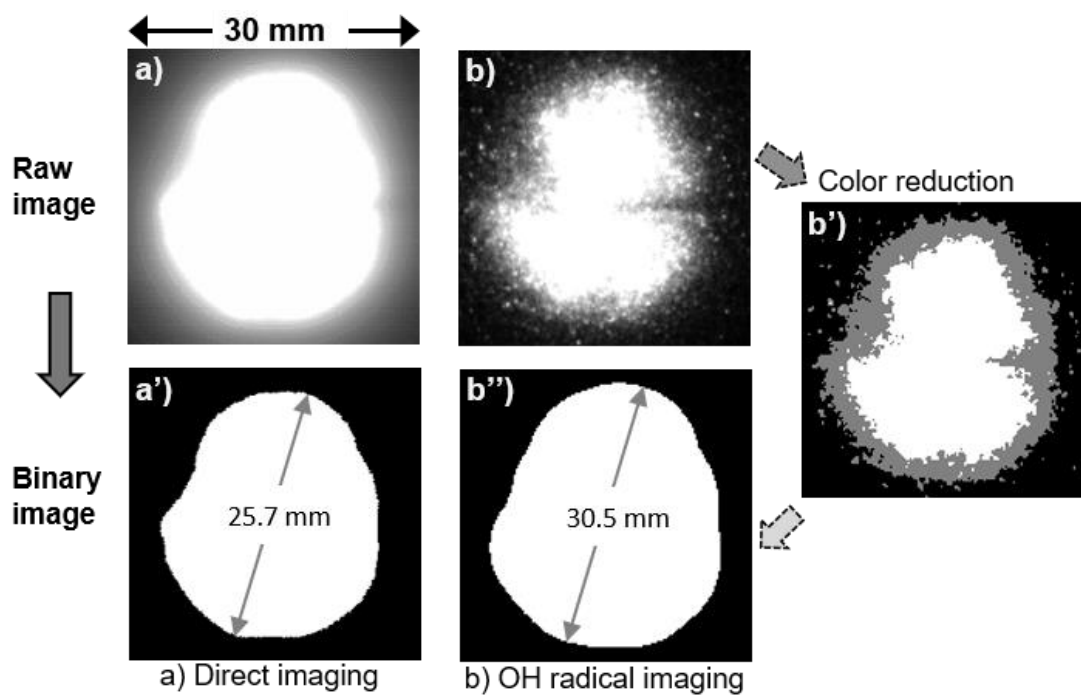


Fig. 2. Raw flame images of ammonia/coal particle cloud co-combustion transformed to binary images.

1. Ms. Ref. No.: PROCI-D-19-00715R1
 2. Author (s) : Khalid Hadi, Ryo Ichimura, Genya Hashimoto, Yu Xia, Nozomu Hashimoto, Osamu Fujita
 3. Title: Effect of fuel ratio of coal on the turbulent flame speed of ammonia/coal particle cloud co-combustion at atmospheric pressure.
- Proceedings of The Combustion Institute

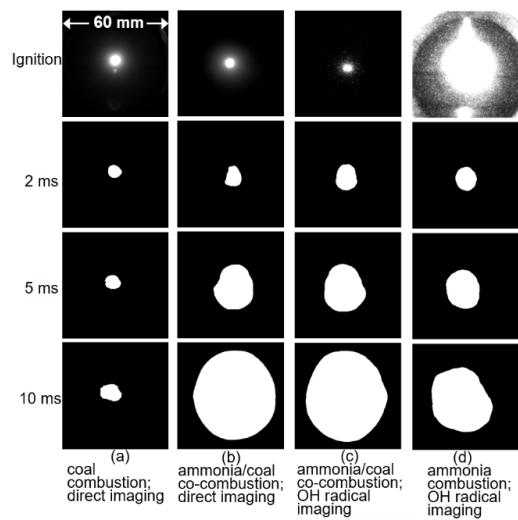


Fig. 3. The sequence of flame propagation images of pure coal, ammonia/coal particle co-combustion, and pure ammonia combustion, at $u' = 0.32$ m/s.

1. Ms. Ref. No.: PROCI-D-19-00715R1
 2. Author (s) : Khalid Hadi, Ryo Ichimura, Genya Hashimoto, Yu Xia, Nozomu Hashimoto, Osamu Fujita
 3. Title: Effect of fuel ratio of coal on the turbulent flame speed of ammonia/coal particle cloud co-combustion at atmospheric pressure.
- Proceedings of The Combustion Institute
-

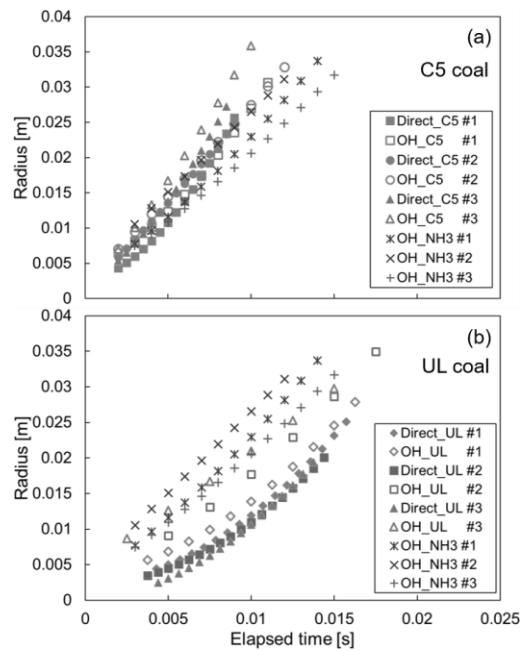


Fig. 4. Flame radius as a function of elapsed time of ammonia/coal particle cloud co-combustion for C5 and UL coal, and pure ammonia combustion, at $u' = 0.65$ m/s. #1, #2 and #3 indicate the experimental numbers of repeated tests.

1. Ms. Ref. No.: PROCI-D-19-00715R1
2. Author (s) : Khalid Hadi, Ryo Ichimura, Genya Hashimoto, Yu Xia, Nozomu Hashimoto, Osamu Fujita
3. Title: Effect of fuel ratio of coal on the turbulent flame speed of ammonia/coal particle cloud co-combustion at atmospheric pressure.

Proceedings of The Combustion Institute

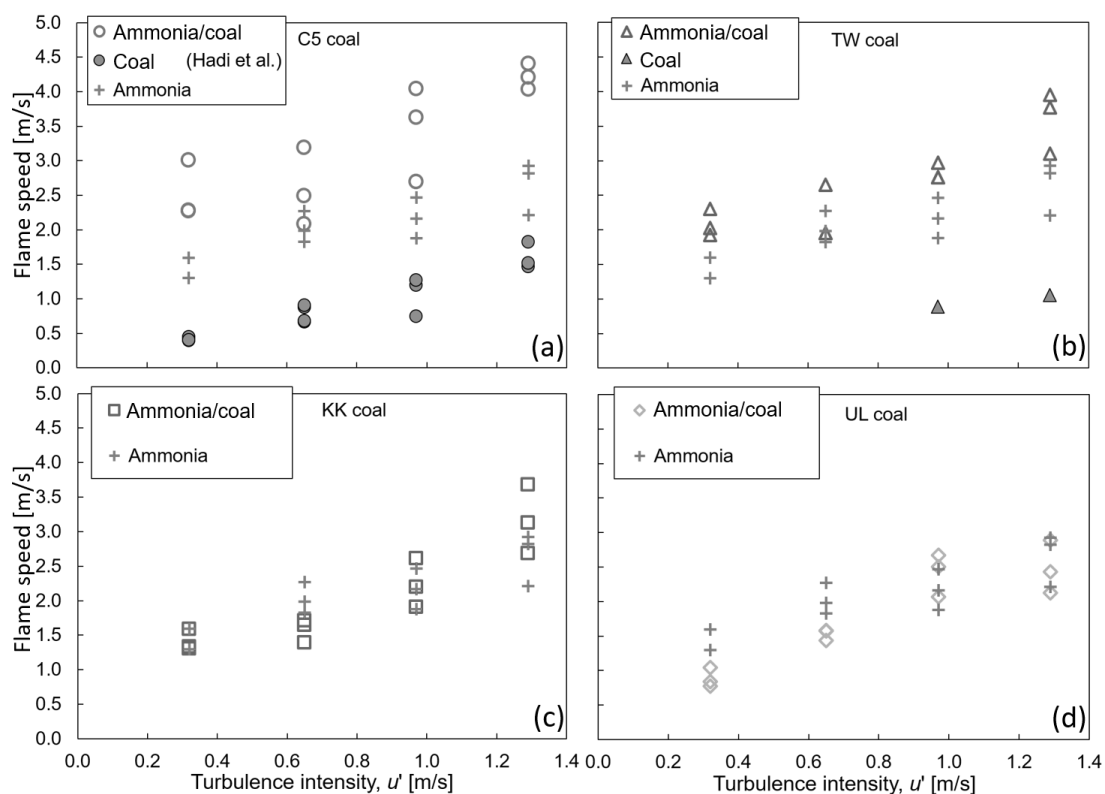


Fig. 5. Relationship between flame speed and turbulence intensity, u' of ammonia/coal particle cloud co-combustion, pure coal, and pure ammonia combustion.

1. Ms. Ref. No.: PROCI-D-19-00715R1
2. Author (s) : Khalid Hadi, Ryo Ichimura, Genya Hashimoto, Yu Xia, Nozomu Hashimoto, Osamu Fujita
3. Title: Effect of fuel ratio of coal on the turbulent flame speed of ammonia/coal particle cloud co-combustion at atmospheric pressure.

Proceedings of The Combustion Institute

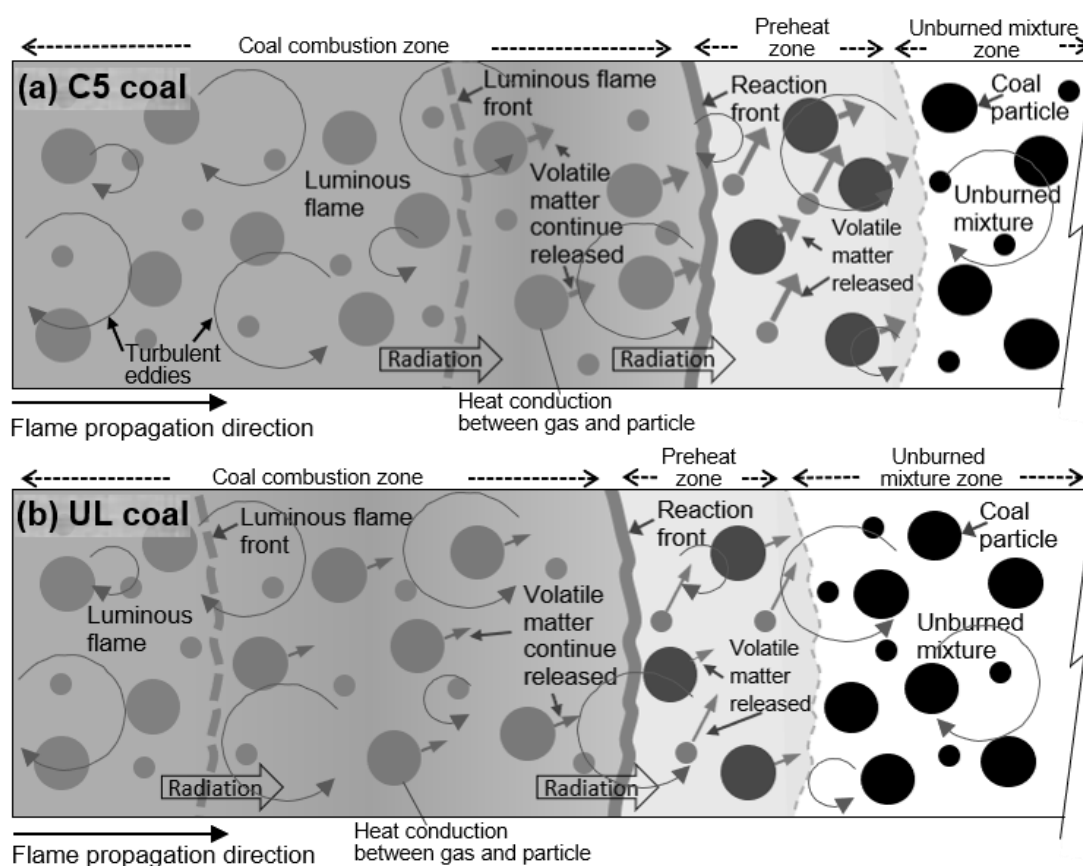


Fig. 6. A mechanism of flame propagation of ammonia/coal particle cloud co-combustion.

1. Ms. Ref. No.: PROCI-D-19-00715R1
2. Author (s) : Khalid Hadi, Ryo Ichimura, Genya Hashimoto, Yu Xia, Nozomu Hashimoto, Osamu Fujita
3. Title: Effect of fuel ratio of coal on the turbulent flame speed of ammonia/coal particle cloud co-combustion at atmospheric pressure.
Proceedings of The Combustion Institute

Appendix A.

The present study aims to introduce the ammonia in practical coal-fired boilers, therefore based on thermal input, the equivalent amount of coal particles were subtracted when the ammonia was added. The detailed amounts of coal subtracted and coal concentrations for all conditions are listed in the following Table S1.

Table S1
Final coal concentration for ammonia/coal particle cloud co-combustion.

Substance	Lower Heating Value of coal (LHV) [MJ/kg]	Amount of coal for $G = 0.6$ kg/m ³ [kg]	Thermal input from coal, $G = 0.6$ kg/m ³ [MJ]	Thermal input from ammonia, $\phi = 0.6$ [MJ]	Needed thermal input from coal if add ammonia [MJ]	Coal subtracted if add ammonia [kg]	Coal subtracted if add ammonia [%]	Final coal concentration for co-combustion [kg/m ³]
Coal (C5)	27.8	0.003714	0.103249	0.021221	0.0820279	0.0007634	20.5535	0.4767
Coal (TW)	27.2	0.003714	0.101021	0.021221	0.0797995	0.0007802	21.0069	0.4740
Coal (KK)	30.1	0.003714	0.111791	0.021221	0.0905701	0.0007050	18.9829	0.4861
Coal (UL)	27.2	0.003714	0.101021	0.021221	0.0797995	0.0007802	21.0069	0.4740
Ammonia	18.6	-	-	0.021221	-	-	-	-